



Analysis of de Haas-van Alphen Oscillations and Band Structure of an Organic Superconductor, θ -(BEDT-TTF) $_2$ I $_3$

Masafumi TAMURA*, Haruo KURODA**, Shinya UJI¹,
Haruyoshi AOKI¹, Madoka TOKUMOTO², A. G. SWANSON^{3,***},
J. S. BROOKS³, C. C. AGOSTA^{4,****} and S. T. HANNAHS⁴

*Department of Chemistry, Faculty of Science,
The University of Tokyo, Hongo, Bunkyo-ku, Tokyo 113*

¹*National Research Institute for Metals,
Nakameguro 2-3-12, Meguro-ku, Tokyo 153*

²*Electrotechnical Laboratory, Umezono, Tsukuba, Ibaraki 305*

³*Department of Physics, Boston University,
Boston, MA 02215, USA*

⁴*Francis Bitter National Magnet Laboratory,
Massachusetts Institute of Technology, Cambridge,
MA 02139, USA*

(Received August 13, 1993)

Analysis of the temperature and field dependence of the de Haas-van Alphen oscillations in an organic superconductor θ -(BEDT-TTF) $_2$ I $_3$ is presented. The cyclotron masses are estimated to be $2.0m_e$ and $3.6m_e$ for slow and fast oscillations, respectively. The indication of magnetic breakdown effect is discussed in terms of the geometry of the Fermi surface. The result is compared with those of the infrared reflectance spectra and the empirical tight-binding band calculations.

[BEDT-TTF, organic superconductor, de Haas-van Alphen effect, cyclotron mass, magnetic breakdown, Fermi surface]

§1. Introduction

The recent advances in the Fermi surface (FS) study in the molecular based organic conductors, BEDT-TTF (bis (ethylenedithiolo) tetrathiafulvalene) salts in particular, have presented sophisticated physical pictures of the electronic structures of these materials.¹⁾ This has been provided by the observation of the magneto-quantum oscillation effects, the de Haas-van Alphen (dHvA) and the Shubnikov-de Haas (SdH) effects. The most

outstanding trend is the experimental supports for the geometry of the two-dimensional (2D) FS predicted by the simple empirical tight-binding calculations based on the frontier molecular orbitals. For the complete analyses of the band structures, however, not only the geometry and topology of FS but also the cyclotron mass should be examined.

A quasi-2D organic conductor θ -(BEDT-TTF) $_2$ I $_3$ is an ambient pressure superconductor with $T_c=3.6$ K.^{2,3)} The arrangement of BEDT-TTF molecules in the donor sheets of this salt⁴⁾ contains no distinct dimerization; it should be distinguished from the dimer-based structures of the β - and κ -type salts. The donor sheets of θ -(BEDT-TTF) $_2$ I $_3$ has approximately high symmetry so as to afford a considerably simple band structure with a large 2D free-electron-like Fermi surface.⁴⁾ However, the situation becomes somewhat complicated when the doubled periodicity

* Present address: The Institute for Solid State Physics, The University of Tokyo, Roppongi, Minato-ku, Tokyo 106.

** Present address: Science University of Tokyo, Yamazaki 2641, Noda, Chiba 278.

*** Present address: AT&T Bell Laboratories, Murray Hill, NJ 07974, USA.

**** Present address: Clark University, Worcester, MA 01610, USA.

stemming from the I_3 anion arrangement⁵⁾ is taken account of. First, most crystals are twinned.^{4,5)} This may yield ambiguity in the experimental study of this salt. Second, a band structure calculated on the basis of the detailed crystal structure gives complex features in the FS geometry; the FS comprises three types of closed portions on the boundary of the first Brillouin zone (BZ).⁶⁾ One of such portions has very small cross-section. Such a feature is sensitive to the empirical parameterization used in the band calculation and should be checked by experiments.

In previous papers,⁷⁻¹⁰⁾ we have reported the first observation of “saw-tooth” dHvA oscillation in θ -(BEDT-TTF)₂I₃. This directly shows that a satisfactorily clean quasi-2D electron system in fact exists in this salt. Two types of dHvA oscillations were recorded: the fast one appearing above about 15 T and the slow one, corresponding to about 100% and 20% of the cross-section of the first BZ, respectively.⁷⁾ The fast one is accompanied by the higher harmonics up to the fourth.⁷⁾ The appearance of the fast oscillation has been interpreted as a result of magnetic breakdown (MB) effect.⁷⁻¹⁰⁾ This supports the view that the FS of this salt consists of a closed pocket and a pair of open portions which are separated from each other by a small gap; it is not likely to think of the three well separated closed portions.

To understand what affords such a band structure and how it is related to other observations, *e.g.* the angle-dependent oscillation of magnetoresistance,¹¹⁾ the values of the cyclotron masses are important. However, the twinning nature of the sample have made it difficult to analyze some of the data on the temperature dependence of the oscillations. Nevertheless, we have separated of the contribution from each twinned domain. In this paper, we report the results of this analysis. In the light of the MB effect and the cyclotron masses, we discuss the geometry of the FS and the band model of this salt.

§2. Experimental

Crystals of θ -(BEDT-TTF)₂I₃ were prepared by the electrochemical method described before.^{3,12)} The crystal does not always exhibits superconductivity.^{3,13)} The sample was

installed in a ³He cryostat designed to operate in high field magnets at Francis Bitter National Magnet Laboratory at The Massachusetts Institute of Technology. The magnetization of the sample was measured by the small-sample force magnetometer.¹⁴⁾ The resistivity was measured by the standard four-probe method with gold contacts using a lock-in ac detection.

§3. Results

Figure 1 shows the magnetization as a function of magnetic field at the selected temperatures.¹⁵⁾ The data was recorded for the crystal other than the one previously reported.⁷⁻¹⁰⁾ A significant difference between these two samples is the appearance of the nodes at about 12, 15 and 20 T in the data in Fig. 1. The Fourier transform of the data displayed in Fig. 2, shows that these nodes result from the beat of the two close frequency components at $f'_1 = 4440$ T and $f'_2 = 4494$ T. The coexistence of such two fast oscillations, corresponding to approximately 100% of the first BZ, in an exactly single crystal contradicts to the basic chemical architecture of the salt. As mentioned above, θ -(BEDT-TTF)₂I₃ often crystal-

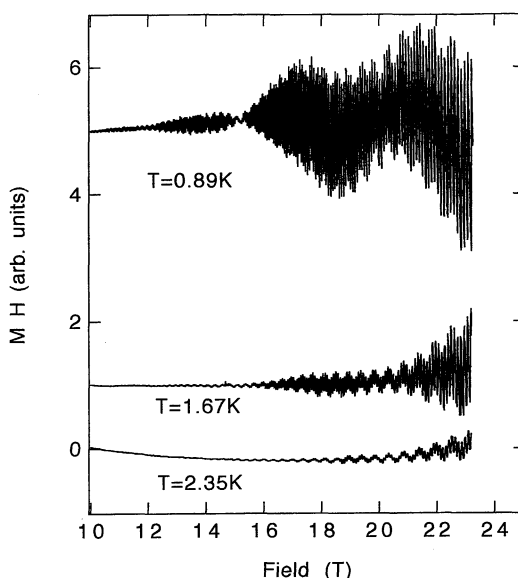


Fig. 1. dHvA oscillations θ -(BEDT-TTF)₂I₃ as a function of field at selected temperatures. The curves for $T=0.89$ K and $T=1.67$ K are shifted up for clarity. Twin effect can be seen as the nodes at about 12, 15 and 20 T.

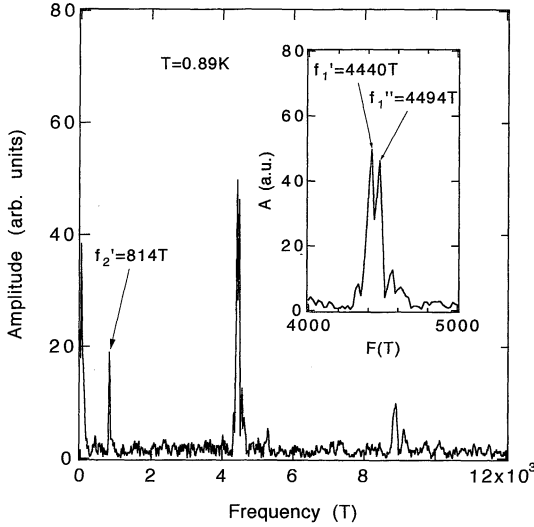


Fig. 2. Fourier transform of the 0.89 K data in Fig. 1. The inset is the blow-up around the higher frequencies.

lizes in a twinned form. Therefore, it is very likely to think of the beat as a result of the twinning in the crystal examined. If this is the case, the nodes due to this beat should be observed at the field, H_n , satisfying,

$$\cos [\pi(f_1'' - f_1')/H_n] = 0, \quad (n=0, 1, 2, \dots) \quad (1)$$

or,

$$(f_1'' - f_1')/H_n = n + 1/2. \quad (n=0, 1, 2, \dots). \quad (2)$$

Corresponding to $n=3$ and 4 , the fields $H_n=15.4$ and 12.0 T are respectively obtained, which is consistent with the observation. The oscillation without such beat was able to be observed for the other crystal⁷⁻¹⁰ (Fig. 3). On the other hand, beat behavior may come from small warping of a single cylindrical FS. The beat having such origin should give nodes at the field, H'_n , satisfying,

$$\cos [\pi(f_1'' - f_1')/H'_n - \pi/4] = 0, \quad (n=0, 1, 2, \dots) \quad (1')$$

or,

$$(f_1'' - f_1')/H'_n = n + 3/4, \quad (n=0, 1, 2, \dots) \quad (2')$$

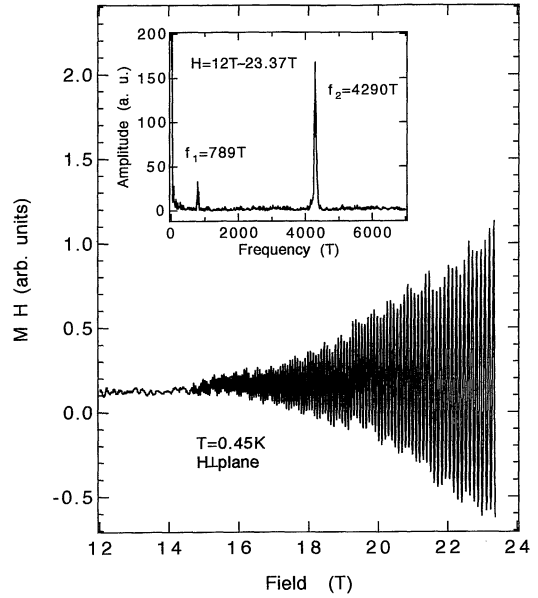


Fig. 3. dHvA oscillations and their Fourier transform (inset) of θ -(BEDT-TTF)₂I₃ showing no distinct beat.

where f_1' and f_1'' correspond to the minimum and maximum of the cross-sectional area of the warped FS, respectively. For $n=3$ and 4 , we obtain $H'_n=14.4$ and 11.4 T, respectively. These values are appreciably lower than those observed for θ -(BEDT-TTF)₂I₃. Thus we conclude that the observed behavior are composed of the contributions from two domains in different orientations; each domain exhibits the fast and slow oscillations, f_1 and f_2 at about 4000 T and 800 T, respectively.

We derive the cyclotron mass values from the data showing the twin effect (Figs. 1 and 2) below, because only they are available for the analysis of the temperature dependence. The inset of Fig. 3 displays the Fourier transform of the magnetization data without a remarkable beat, showing the fast oscillation at $f_1=4290$ T. Assuming that the field direction was parallel to the principal axis in this measurement, we can estimate the inclination of each twinned domain with respect to the field from the deviation of f_1' and f_1'' from f_1 . The angles between the principal axes of the domains and the field direction are 15° and 17° , corresponding to f_1' and f_1'' , respectively. This misorientation may yield at most 6% of error in our mass analysis for a cylindrical FS.

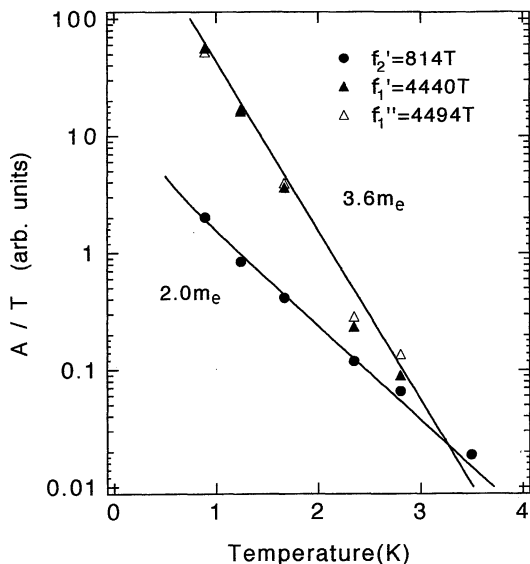


Fig. 4. The mass-plot, the plot of A/T versus T , where A is the amplitude of the Fourier component at each frequency.

In Fig. 4, the so-called mass-plot, the plot of A/T versus T , is shown, where A is the amplitude of the Fourier component at each frequency. From the slope of each plot, the cyclotron masses are evaluated. For the fast oscillations, $m_1 = 3.6 m_e$, and for the slow oscillation, $m_2 = 2.0 m_e$.

Field dependence of the oscillation amplitude is also analyzed in terms of the Lifshitz-Kosevich (LK) formula.¹⁶⁾ In the presence of the MB effect, the tunnelling probability is approximately expressed as,

$$P = \exp(-H_B/H), \quad (3)$$

where H_B denotes the breakdown field. We consider here the tunnelling junctions between the closed pocket (orbit 2) and the pair of open portion. Such a situation modifies the original LK formula for a single orbit. The results can be expressed as,¹⁷⁾

$$S_1 = M_1(H) H^{1/2} \sinh [K(m_1/m_e) T/H] \propto P^4 \exp[-K(m_1/m_e) T_{D1}/H], \quad (4)$$

and,

$$S_2 = M_2(H) H^{1/2} \sinh [K(m_2/m_e) T/H] \propto (1-P)^2 \exp[-K(m_2/m_e) T_{D2}/H], \quad (5)$$

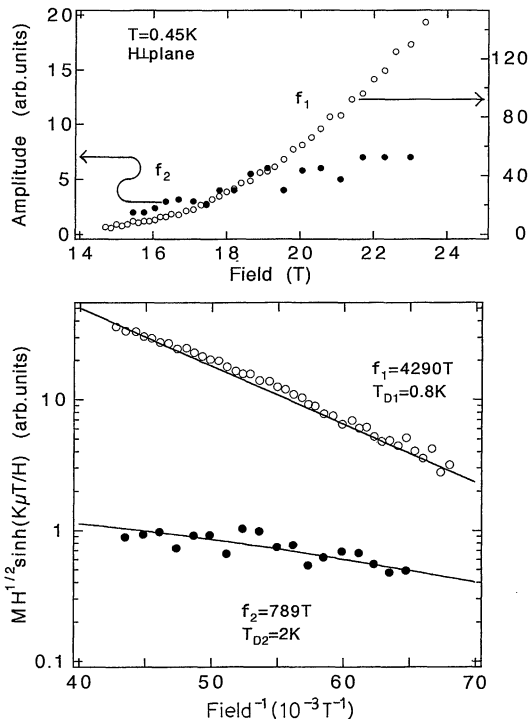


Fig. 5. Top: Field dependence of the oscillation amplitude. Bottom: The Dingle plot of the data in Fig. 3. The solid lines stand for the calculations considering the magnetic breakdown effect.

where $K = 2\pi^2 m_e c k_B / e \hbar = 14.7 \text{ T/K}$, $M(H)$ is the amplitude of the oscillation, and T_D is the Dingle temperature; the subscripts, 1 and 2, denote the fast and slow oscillations, respectively. By using m_1 and m_2 evaluated as above, T_{D1} , T_{D2} and H_B can be estimated from the slope of $\log(S)$ versus $1/H$ plots. Figure 5 shows such a plot of the data given in Fig. 3. Too small amplitude of the oscillations below 15 T prevent us from evaluating the parameters precisely. Nevertheless, the parameter set $T_{D1} = 0.8 \text{ K}$, $T_{D2} = 2 \text{ K}$, and $H_B = 15 \text{ T}$ seems to reproduce the data well, as depicted by the solid curves in Fig. 5. The overall field dependence is thus explained by the MB effect.

Another evidence for the MB effect is the overall field dependence of the resistivity.¹⁵⁾ Figure 6 shows the transvers magnetoresistance of θ -(BEDT-TTF)₂I₃ at 0.7 K for the field perpendicular to the basal plane. SdH oscillation appears above about 15 T. Superconductivity was not observed for this

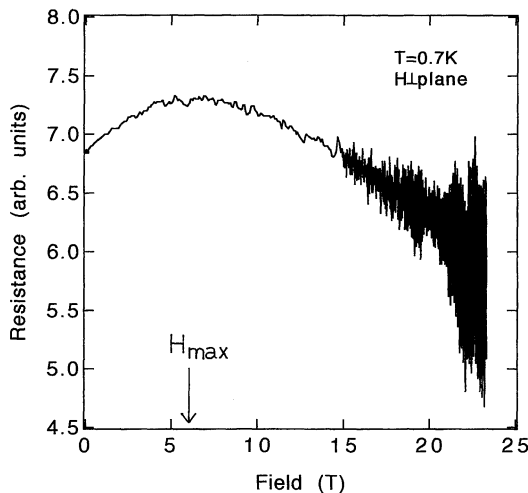


Fig. 6. Transverse Magnetoresistance of θ -(BEDT-TTF)₂I₃ at 0.7 K. The field was applied perpendicular to the two-dimensional plane.

sample. The low field behavior is consistent with that reported in ref. 11. Noteworthy is the maximum around 6 T.

By taking account of the MB effect, the decrease in resistance above $H_{\max}=6$ T can be qualitatively explained as follows. In the low field limit, $H \ll H_B$, where the MB effect is negligible, the resistivity is dominated by the electron scattering. The resistivity should increase quadratically until the MB effect becomes appreciable. In the high field limit, the dominant term in the resistivity can be calculated by means of a path integral method including the possibility of the magnetic breakdown. This contribution is written as,¹⁷⁻¹⁹⁾

$$R = (H/nec)8(1-P)/\pi P, \quad (6)$$

where n is the number density of the carriers. This term takes the form $1 + H_B/2H$ as $H \rightarrow \infty$, so that the resistivity decreases with increasing field. Hence, a maximum of resistivity should appear at an intermediate field, H_{\max} , which depends on H_B and the scattering time. Such behavior has been found also for (BEDT-TTF)₂KHg(SCN)₄,²⁰⁾ which has FS topology similar to that of θ -(BEDT-TTF)₂I₃. According to the semiclassical model assuming a field independent scattering time, H_{\max} lies between $H_B/3$ and $H_B/10$.¹⁸⁾ Our results, $H_B=15$ T and $H_{\max}=6$ T, can be qualitatively

explained by this scheme.

§4. Discussion

The intermolecular transfer interactions in the donor sheets of θ -(BEDT-TTF)₂I₃ can be categorized into two groups; there are three face-to-face ones and four face-to-side ones.⁶⁾ The difference within each group is related to the structural modulation on the uniform packing of BEDT-TTFs arising from I₃⁻ ion arrangement. Since this modulation is expected to be small, we first consider only two types of transfer integrals, t_{f-f} and t_{f-s} , standing for the two groups in describing the band structure. This simplification enable us to treat the Fermi surface geometry and other physical properties exactly. In this picture, the open and closed portions of FS stick together at the MB junctions. The geometry of the FS is determined only by the ratio of the transfer integrals, t_{f-f}/t_{f-s} .

On the basis of such approximation, the infrared reflectance spectra of this salt was first analyzed and the band structure was deduced.^{21,22)} The ratio of the transfer integrals, t_{f-f}/t_{f-s} , found to reproduce the optical results, is 0.59.²¹⁾ From the reported band parameters,²¹⁾ the cyclotron mass corresponding to the orbit on each portion of FS can be calculated by use of the following equations,

$$m_c = (\hbar^2/2\pi)(\partial A_c/\partial \epsilon); \quad \epsilon = \epsilon_F \quad (7)$$

and,

$$(\partial A_c/\partial \epsilon) = S_{BZ} \rho_c(\epsilon); \quad \epsilon = \epsilon_F \quad (8)$$

where m_c and A_c are the mass and cross sectional areas for the cyclotron orbit c , S_{BZ} the area of the first BZ, and $\rho_c(\epsilon_F)$ density of states per 2D unit cell per spin for the portion of FS corresponding to the orbit c . It is also possible to estimate the cross sectional areas. The cyclotron masses thus calculated are, $m_1=2.2 m_e$ and $m_2=1.0 m_e$, with the cross sectional areas, A_1 and A_2 , 100% (exact) and 14% of S_{BZ} , respectively. Here, $c=1$ and $c=2$ denote the whole FS and the closed portion, respectively (Fig. 7).

Equations (7) and (8) indicate that the cyclotron mass for a 2D system is proportional to the (partial) density of states of the relevant portion of the Fermi surface. It follows from

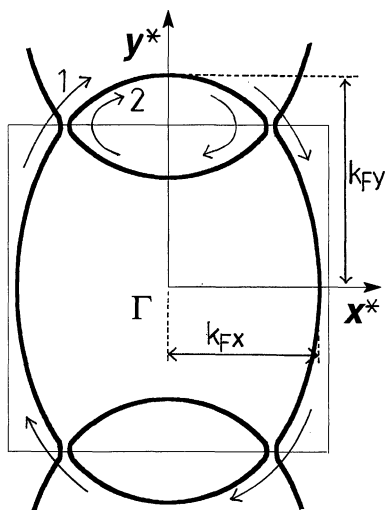


Fig. 7. The Fermi surface topology concluded in this study, together with the notation of the cyclotron orbits, 1 and 2. The directions, x and y , corresponds to the b and a axes in the monoclinic lattice defined in ref. 4, respectively.

this that the larger cyclotron mass value for the fast oscillation arising from the MB effect is the simple sum of the partial densities of states of the portions to be coupled each other by the breakdown; it is not an average along the coupled orbit. Therefore, for a coupled large orbit composed of a closed pocket and open portions, we usually obtain cyclotron mass value larger than that for the small pocket only. The larger value of the coupled orbit mass, as in the present case, is not surprising and does not necessarily involve the larger mass for the open portions. We have to be careful in comparing the cyclotron masses for different types of orbits. The enhanced mass for the open portions of the FS larger than that for the coupled orbit²³⁾ cannot be concluded.

The geometry of the FS concerns the two ratios, m_1/m_2 and A_2/A_1 . The values, $m_1/m_2=2.2$ and $A_2/A_1=0.14$, are inferred from the optical results, while the dHvA oscillations give $m_1/m_2=1.8$ and $A_2/A_1=f_2/f_1=0.18$. This comparison supports the picture shown in Fig. 7, although there remains discrepancy which probably comes from the simplification introduced in the analysis of the optical data. The MB effect clearly shows opening of a

small gap at the junction of FS. This gap should give rise to interband optical transitions. However, the transition energy, i.e. the gap width, is so small that this interband contribution cannot be well separated from the intraband one in the observed spectra. In ref. 21, therefore, the band parameters were estimated from the plasma frequencies including the low energy interband contributions. Since the FS is still connected along the x -direction in Fig. 7 even in the presence of the gap, such overestimation of the plasma frequency is expected mainly for the y -direction data. This means that k_{Fy} in Fig. 7 is relatively underestimated, which results in the underestimation of m_2 and A_2 in the analysis of the optical data. The discrepancy between the optical and the dHvA results can be qualitatively explained in this way.

On the other hand, the values of cyclotron mass, $m_1=3.6 m_e$, deduced from the dHvA oscillations is larger than that calculated from the optical results by the factor of about 1.6. In order to remove this discrepancy, the transfer integrals smaller than the reported ones^{21,22)} by the factor of 0.6 should be used. Such difference cannot be ascribable only to experimental error. It is also difficult to explain this by taking account of the difference in the transfer integrals within each group. Mass enhancement near the Fermi level due to many-body effect, such as electron-phonon interaction, is thereby suggested. The optical spectra probe the global structure of the conduction band rather than the detailed features near the Fermi level, so that the optical mass is insensitive to the many-body effect on the quasiparticle energy near the Fermi level.

Next, let us direct our attention to the gap affording the MB effect. The breakdown field, H_B , is approximately related to the energy gap near the junction, ϵ_g , by the equation,^{17,24)}

$$H_B = (\pi/4)(c/e\hbar)(\epsilon_g^2/v_x v_y), \quad (9)$$

where v_x and v_y are the components of the Fermi velocity at the junction parallel and perpendicular to the zone boundary, respectively. The simplified tight-binding model with the parameters inferred from the optical results²¹⁾ yields $v_x=1.5 \times 10^7$ cm/s and $v_y=1.1 \times 10^7$ cm/s. From this, together with $H_B=15$ T, it

follows that $\varepsilon_g = 1.5 \times 10^{-2}$ eV. If the mass enhancement near the Fermi level is taken into account, the gap should be about the half of this value. A more popular formula,¹⁷⁾

$$H_B \sim (m_2 c / e \hbar) (\varepsilon_g^2 / \varepsilon_F) \quad (10)$$

with the cyclotron mass, $m_2 = 3.6 m_e$, results in the same order of magnitude, i.e. $\varepsilon_g \sim 1 \times 10^{-2}$ eV. The corresponding spacing between the open and the closed portions of the FS at the junction is as small as about 2% of π/b , where b is the lattice constant along the x -direction. This justifies the application of the simplified band model to approximate estimation of the masses and ε_F .

In the framework of the tight-binding band model, the origin of the gap at the zone boundary is the difference of transfer integrals within the groups, which reflects the small deviations from the uniform packing of BEDT-TTFs. In the present case, it seems difficult to predict such a small energy structure accurately enough. Nevertheless, the empirical tight-binding band calculations can provide a reasonable estimation of the order of magnitude of the gap.⁶⁾ Another problem which exists in the present case is the failure in prediction of the topology of FS by the calculations.⁶⁾ Even in the presence of the deviations from the uniform packing, the geometry of FS is basically determined by the ratio of the group averages of the transfer integrals, $\langle t_{f-f} \rangle / \langle t_{f-s} \rangle$. Since the modes and characters of the intermolecular contacts are entirely different between the groups, attention should be paid in comparing t_{f-f} with t_{f-s} . The calculations⁶⁾ yielded $\langle t_{f-f} \rangle / \langle t_{f-s} \rangle = 1.7$, while the optical and the dHvA experiments support $\langle t_{f-f} \rangle / \langle t_{f-s} \rangle = 0.59$. The former one is sensitive to the details in the parameterization in the extended Hückel molecular orbital calculations, and can be suppressed down to about 0.2 by taking account of the contributions of sulfur $3d$ orbitals.²⁵⁾ Therefore, the contradiction between the experiments and the calculations is expected to be removed, when moderate weight of the sulfur $3d$ contributions is adopted. In spite of such arbitrariness in the empirical parameterization, it is evident that in studying the electronic structures of the molecular conductors the framework of the tight-binding

band model works well with the help of experiments, as demonstrated in this study.

§5. Conclusion

From the analysis of the dHvA oscillations in θ -(BEDT-TTF)₂I₃, the cyclotron masses have been evaluated to be $2.0 m_e$ and $3.6 m_e$, for the slow and fast oscillations, about 800 T and 4000 T. The latter has been shown to be as a consequence of the magnetic breakdown effect which connects the closed and open portions of the Fermi surface. These two portions are separated by the gap of 1.5×10^{-2} eV at the junction. These results are consistent with the topology of the Fermi surface deduced from the tight-binding band model with the parameters inferred from the optical measurement.

Acknowledgments

We would like to thank the staff of the Francis Bitter National Magnet Laboratory at the Massachusetts Institute for Technology for their assistance in the measurements. We are also indebted to Professor Hayao Kobayashi and Dr. Akiko Kobayashi for informing us of the details of the band calculations. One of the authors (M. Tamura) would like to thank Professor Minoru Kinoshita, Professor Kyuya Yakushi, Professor Reizo Kato and Dr. Hiroyuki Tajima for their enlightening collaboration.

References

- 1) For example, see Synth. Met., 41–43 (1991). (*Proc. of Int. Conf. Science and Technology of Synthetic Metals, Tübingen, 1990.*)
- 2) H. Kobayashi, R. Kato, A. Kobayashi, Y. Nishio, K. Kajita and W. Sasaki: Chem. Lett. 789 (1986).
- 3) M. Tamura, H. Tajima, H. Kuroda and M. Tokumoto: J. Phys. Soc. Jpn. 59 (1990) 1753.
- 4) H. Kobayashi, R. Kato, A. Kobayashi, Y. Nishio, K. Kajita and W. Sasaki: Chem. Lett. 833 (1986).
- 5) A. Kobayashi, R. Kato, H. Kobayashi, S. Moriyama, Y. Nishio, K. Kajita and W. Sasaki: Chem. Lett. 2017 (1986).
- 6) H. Kobayashi, R. Kato, A. Kobayashi, T. Mori, H. Inokuchi, Y. Nishio, K. Kajita and W. Sasaki: Synth. Met. 27 (1988) A289.
- 7) M. Tokumoto, A. G. Swanson, J. S. Brooks, M. Tamura, H. Tajima and H. Kuroda: Solid State Commun. 75 (1990) 439.
- 8) M. Tokumoto, N. Kinoshita, H. Anzai, A. G. Swanson, J. S. Brooks, S. T. Hannahs, C. C.

- Agosta, M. Tamura, H. Tajima, H. Kuroda, A. Ugawa and K. Yakushi: *Synth. Met.* **42** (1991) 2459.
- 9) M. Tokumoto, A. G. Swanson, J. S. Brooks, C. C. Agosta, S. T. Hannahs, N. Kinoshita, H. Anzai, M. Tamura, H. Tajima, H. Kuroda and J. R. Anderson: in *Organic Superconductivity*, ed. V. Z. Kresin and W. A. Little (Plenum Press, New York, 1990) p. 167.
 - 10) M. Tokumoto, A. G. Swanson, J. S. Brooks, C. C. Agosta, S. T. Hannahs, N. Kinoshita, H. Anzai, M. Tamura, H. Tajima, H. Kuroda, A. Ugawa and K. Yakushi: *Physica B* **184** (1993) 508.
 - 11) K. Kajita, Y. Nishio, T. Takahashi, W. Sasaki, R. Kato, H. Kobayashi, A. Kobayashi and Y. Iye: *Solid State Commun.* **70** (1989) 1189.
 - 12) R. Kato, H. Kobayashi, A. Kobayashi, Y. Nishio, K. Kajita and W. Sasaki: *Chem. Lett.* 957 (1986).
 - 13) K. Kajita, Y. Nishio, S. Moriyama, W. Sasaki, R. Kato, H. Kobayashi and A. Kobayashi: *Solid State Commun.* **64** (1987) 1279.
 - 14) J. S. Brooks, M. J. Naughton, Y. P. Ma, P. M. Chaikin and R. V. Chamberlin: *Rev. Sci. Instrum.* **58** (1987) 117.
 - 15) A. G. Swanson: Ph. D. Thesis, Boston University, 1991.
 - 16) I. M. Lifshitz and A. M. Kosevich: *Sov. Phys.-JETP* **2** (1956) 636.
 - 17) D. Shoenberg: *Magnetic Oscillations in Metals* (Cambridge Univ. Press, Cambridge, 1984) Chap. 7.
 - 18) L. M. Falicov and P. R. Sievert: *Phys. Rev. Lett.* **12** (1964) 558.
 - 19) L. M. Falicov, A. B. Pippard and P. R. Sievert: *Phys. Rev.* **151** (1966) 498.
 - 20) S. Uji, H. Aoki, J. S. Brooks, S. J. Klepper, C. C. Agosta, M. Tokumoto, N. Kinoshita, Y. Tanaka, H. Anzai, A. S. Perel, G. J. Athas and D. A. Howe: *Solid State Commun.*, in press.
 - 21) M. Tamura, K. Yakushi, H. Kuroda, A. Kobayashi, R. Kato and H. Kobayashi: *J. Phys. Soc. Jpn.* **57** (1988) 3239.
 - 22) M. Tamura, R. Masuda, T. Naito, H. Tajima, H. Kuroda, A. Kobayashi, K. Yakushi, R. Kato, H. Kobayashi, M. Tokumoto, N. Kinoshita and H. Anzai: *Synth. Met.* **42** (1991) 2499.
 - 23) T. Sasaki, H. Sato and N. Toyota: *Solid State Commun.* **76** (1990) 507.
 - 24) E. I. Blount: *Phys. Rev.* **126** (1962) 1636.
 - 25) A. Kobayashi and H. Kobayashi: private communication.
-